Morphology, Structure and Properties of Electrospun Multi-Walled Carbon Nanotube/Polysulfonamide Composite Nanofibers

Bin-Jie Xin, Wenjie Chen

Shanghai University of Engineering Science, Shanghai CHINA

Correspondence to:
Bin-Jie Xi email: Xiaobo2000@gmail.com

ABSTRACT

In this paper, the morphology, structure and properties of electrospun Polysulfonamide (PSA)/multi-walled carbon nanotubes (MWCNTs) fibers are investigated systematically. The experimental results indicate that the diameter of electrospun PSA fiber increased by the blending of MWCNTs while its crystallinity decreased. Both the conductivity and mechanical properties of PSA/MWCNT fibers were improved by the blending of MWCNTs at a concentration below 5% MWCNT. The thermal behavior of the electrospun fibers was influenced by the MWCNT concentrations through the Thermogravimetric Analysis (TGA).The new developed PSA/MWCNTs composite nanofiber has excellent thermal stability and mechanical properties compared with the usual PSA fibers.

Keywords: Polysulfonamide, Electrospinning, Multi-walled carbon nanotube, thermal reliability

INTRODUCTION

Electrospinning is one of the most frequently used methods for the preparation of various kinds of polymer fibers at the nano-metric scale; a high specific surface area and high porosity can be achieved through this means [1, 2]. Due to its advantages, electro-spun fibers have been widely used for many applications, such as reinforcing materials [3, 4], sensors [5-10], filtering materials[11-13], catalytic carrier [14], luminescent materials [15, 16], individual protection materials [17, 18], biomedical materials (including drug delivery [19, 20], tissue engineering [21-23], and enzyme immobilization [24]). Among these research studies, Wang et al. electrospun polyelectrolyte and located its membrane on a quartz crystal microbalance, fabricating a novel humidity sensor. It was reported that the sensors exhibited high sensitivity [5]. Song et al. combined electrospinning with surfactant-directed assembly approach, preparing sensitive mesoporous ZnO-SnO_2 (m-Z-S) nanofibers. They showed the mesoporous fiber film exhibited high sensitivity, quick response and recovery properties [6]. Desai et al. electrospun Chitosan/PEO blended solutions onto a spun-bonded non-woven polypropylene substrate, fabricating nano-fibrous filter media [12].

Recently, there have been many studies focusing on the development of functional nano composites using the electrospun polymer/nano-particles fibers [25, 26]. Through the electrospinning of the blended polymer and functional particles, some new multifunctional electrospun fibers have been developed. Among these nano particles, carbon nanotube (CNT) is the most promising one, which has attracted a great attention due to its excellent electrical conductivity properties and mechanical properties [27-31]. Zhou et al. used the electrospinning method to prepare PEO (polyethylene oxide) and PVA (polyvinyl alcohol) nanofibers containing MWCNTs (multi-walled carbon nanotubes) and made an investigation of the interaction between MWCNTs and the polymer matrix[32]. Saeed et al. fabricated MWNT/PCL nano composites (multi-walled carbon nanotube/polycaprolactone) where the MWNTs were used as the reinforcing materials [33]. They found the MWNTs can be embedded within the nanofibers and well oriented along the axes of the electrospun nanofibers. Jose et al. synthesized the aligned nanocomposite of Nylon 6 and surface-modified MWNTs through electrospinning [34]. Ra et al. investigated the effect of CNTs on the conductivity of the PAN (polyacrylonitrile) fiber. They found that both the conductivity and morphology of the electrospun fibers can be affected by the CNT concentration [35]. Sen et al. blended the SWCNTs(single walled carbon nanotubes) with the PS (polystyrene) solution and electrospun the PS/

CNTs nano-fibers [36]. In 2009, Saeedeh Mazinani, et al. [26] studied the dispersion of CNTs in the PS initial electrospinning solution and evaluated the electrical properties and mechanical characteristic of the electrospun PS/CNT mats with different CNT contents.

However, very few researches have been reported on the fabricating PSA (Polysulfonamide)/CNT nanofibers. Polysulfonamide (PSA) is one kind of heat-resistant polymer owing to –NHOC, -SO_2- group in its molecular [37-39]. Its LOT (limit oxygen index) is 33 and no melting and shrinking occurs when it is burned, which show the PSA material has excellent flame resistance. Compared to Aramid 1313 polymer, the heat resistance of the PSA is much better. Under the 350 degrees environment, the strength of PSA fiber is reduced to 38% while the Aramid 1313 is destroyed thoroughly. In addition, PSA also shows excellent radiation performance, chemical stability and dying properties. It has obtained a great attention and can be used in many fields like aerospace, high-temperature environments and civil fields with flame retardant requirements. However, the electrical resistance of PSA is high and its breaking tenacity is low, which limit its application in the development of protective textile products.

In our research, the PSA nanocomposite fibers were prepared by the electrospinning method using the PSA solution blended with the different concentrations of MWCNT. The effect of MWCNT on fiber's morphologies and properties including electrical conductivity and mechanical properties were studied qualitatively and systematically.

EXPERIMENTAL

Materials

The materials used in this study include PSA solution (2.0~2.5dl/g intrinsic viscosity and12% weight mass ratio (12wt %) concentration), DMAC (dimethylacetamide) solvent and MWCNTs. These materials above are supplied by Shanghai Tanlon Fiber Co. LTD.

Electo-Spinning

Surface modification technology was employed to improve the dispersion of MWCNT in PSA solution. The MWCNTs were first dispersed using an ultrasonic machine in a mixed solvent of 70% nitric acid and 98% sulfuric acid for 1h. The mixed solvent with MWCNTs was added in an oil bath to reflux and condense at 120 degrees for another 1h and then washed using distilled water repeatedly until the PH of the mixed solution reached 7.0. The surface modified MWCNTs were obtained after drying over 24h.

A calculated amount of treated MWCNTs were dispersed in DMAC using ultrasonic vibration for 30 min, then added into 12% PSA/DMAC solution and stirred mechanically for 0.5h. The MWCNT/PSA composite spinning solutions with different contents were prepared after mechanical stirring for 1h and ultrasonic vibration for 1h. The experimental data are showed in *Table I*.

TABLE I. The specifications of PSA/MWCNTs composite spinning solution.

Sample	PSA /(g)	MWCNTs /g	DMAC /ml
PSA	50	0	0
1wt% MWCNTs / PSA	50	0.0606	1
3wt% MWCNTs / PSA	50	0.1856	3
5wt% MWCNTs / PSA	50	0.3158	5
7wt% MWCNTs / PSA	50	0.4516	7

DMAC: dimethylacetamide

The schematic of electrospinning set-up employed in this work is shown in *Figure 1*. The prepared PSA/MWCNTs solutions were fist injected into a plastic syringe with a stainless steel needle (1.2 mm inner diameter, Changzhou Yuekang Medical Equipment Co. LTD.). A constant volume of the PSA/MWCNTs solution was delivered to the needle at a flow rate of 0.1 m/h using a syringe pump. A high potential of 28 kV provided by a high-voltage generator (Model: ES-203, Shanghai Lingshi Electronic Co. LTD) was used during the spinning of the polymer solution. The prepared nanocomposite fibers were collected on the aluminum foil stuck to a rotating drum with the rotation velocity set to be 42rpm. The drum located at 15cm distance from the needle tip was connected to the ground.

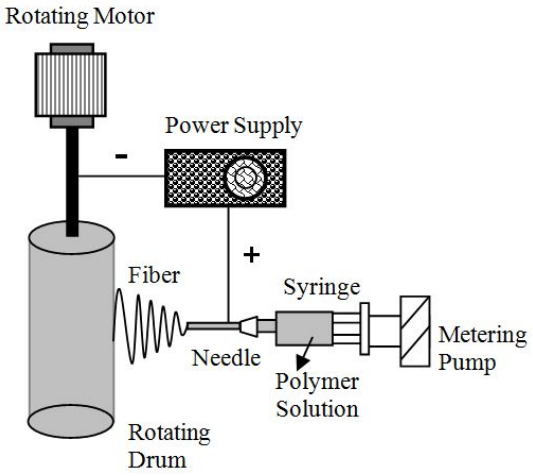

FIGURE 1. System set-up of the electro-spinning unit for manufacturing PSA fibers.

Measurements and Characterization

The morphology and the MWCNT distribution in the PSA/MWCNTs composite nanofibers were investigated using SEM (S-3400N) and TEM (J1OL JEM-2100). X-ray diffraction (XRD) (k780FirmV_06) using Cuka radiation (λ=0.154nm) was employed to measure the crystallinity of fibers with the Bragg angle (2θ) ranging from 5° to 90°. The XRD experiments were performed at 40kV and 40mA, with a scan rate of 0.8°/step. Fourier transform infrared (FTIR) spectra were conducted using AVATAR 370 FR-IR spectrometer.

The conductivity of PSA/MWCNTs nanocomposite fibers with different MWCNT concentrations were measured using both ZC26 (Shanghai AnBiao electronic co., LTD) and UT70A conductivity meter (Shanghai YiZhu electric co., LTD). Five electrospun fibrous mats with 10cm×10cm in size of each sample were prepared and measured.

A single fiber mechanical tester (YG006) was employed to measure the mechanical properties of fibers. Each sample with dimensions of 150mm and 5mm (length and width) after a standard conditioning were weighted and measured 10 times. The extension rate was set to be 10 mm/min at room temperature.

Thermogravimetric analysis (STA PT-1000, Germany) was used to characterize the thermal behaviors of the PSA/MWCNTs fibers. For each sample, 15 mg of PSA fibers was loaded in a platinum pan and heated at a rate of 20℃/min from room temperature to 700℃ at the nitrogen environment with the gas flow set to be 80-100 L/min.

RESULTS AND DISCUSSION

Scanning Electron Microscope (SEM)

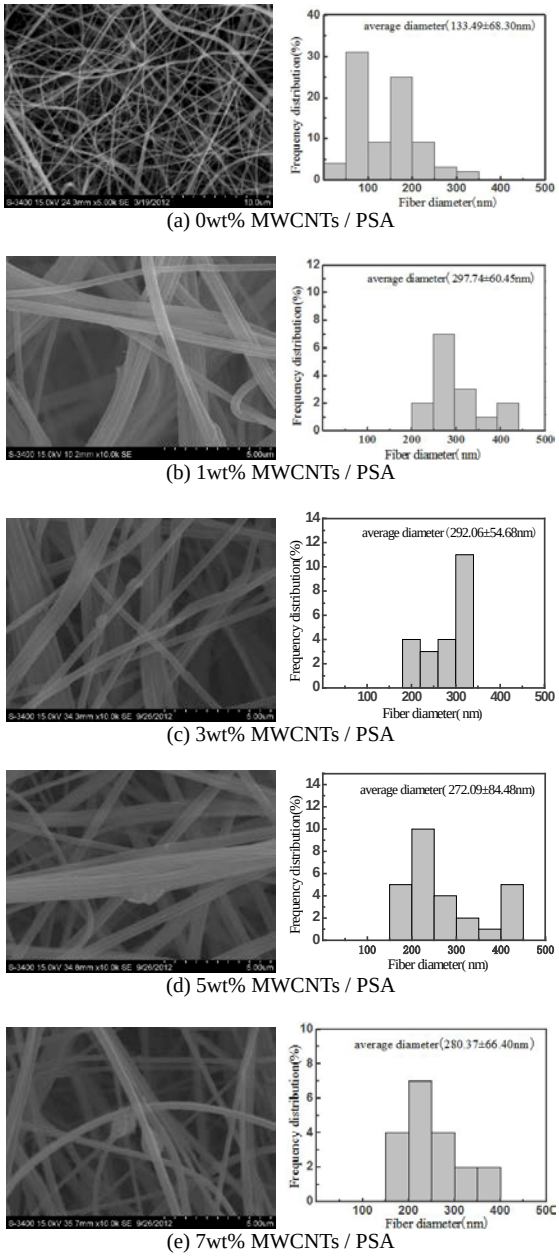

FIGURE 2. SEM images and diameter distribution of 12% PSA electrospun fibers with different MWCNT concentrations.

Figure 2a-e illustrates the morphological features of PSA/MWCNTs nanocomposite fibers with different MWCNT concentrations. As depicted, the blending of MWCNTs can lead to an increase of the average fiber diameter and a more roughly fiber surface. The reason is that the blending of MWCNTs can increase the viscosity of the PSA solution, so as to increase the resistance of fiber drawing from polymer matrix.

However, it is interesting to find that there is a slight decrease of fiber average diameter as the MWCNT concentration is increased from 1% to 5%. The addition of MWCNT enhanced the conductivity of polymer due to its excellent conductivity. When the MWCNT concentration below 5%, no large agglomerates have been found in the blending polymer system and a conductive network can be formatted gradually as the MWCNT concentration increasing, thus the tension acted on jet is increased and it favors the formation of thinner fibers. Baumgarten et al [40] suggested that the fibers diameter is highly correlated to the cubic root of the conductivity of the spinning solution. However, when the concentration of MWCNT was increased further, large agglomerates can be found (over 6mm in scale), it thus limits the conductivity performance of MWCNTs and the formation of the integrated conductive network. Therefore, the spinning tension is decreased and the average diameter of fibers is increased accordingly as illustrated in *Figure 2e*.

Transmission Electron Microscopy (TEM)

TEM was employed to evaluate the dispersion of MWCNT in fibers. *Figure 3* illustrates the PSA/MWCNT fibers with 3% MWCNTs.

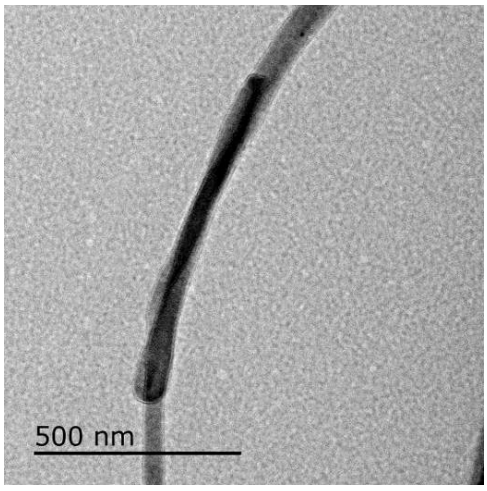

FIGURE 3. TEM images of MWCNTs/PSA electrospun fibers with 3% MWCNTs.

As illustrated in *Figure 3*, MWCNTs can be arranged along the PSA fiber axial when the concentration of MWCNTs was 3%. Two main factors may affect the dispersion of MWCNTs in PSA matrix. First, MWCNTs used in this work were treated by acid and there were many –OH– hydrophilic groups on their surface, leading to a close connection with PSA matrix. Second, ultrasonic vibration was employed to disperse MWCNTs. Local high temperature and atmospheric pressure could be produced by the ultrasonic cleaner, it contributes to the effectively dispersing the MWCNTs in matrix.

XRD Analysis of PSA/MWCNTs Nanofibers

As shown in *Figure 4*, the blending of MWCNTs affected the crystallinity of fibers considerably. The curve of the Electrospun PSA fibers has a peak at about 22.15°, which indicates that there are still some of macromolecules orderly aligned although no integrated crystals appears. However, the peak at 22.5° is found to be disappeared after adding MWCNTs into PSA matrix, which illustrates that the addition of MWCNTs decreases the crystallinity of the blended fibers [46, 47]. Some literatures have reported that MWCNTs can act as a nucleation agent which can improve the crystallinity of fibers. However, MWCNTs hindered the movement of polymer matrix's molecular chains, which limits the crystal growth on the other side.

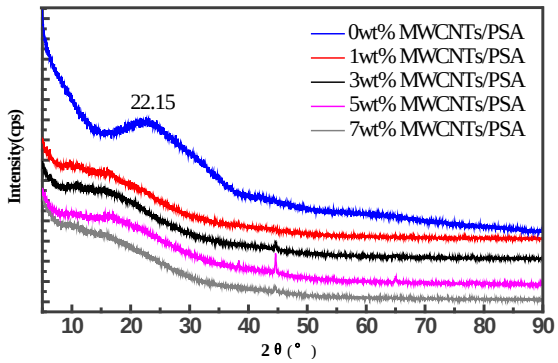

FIGURE 4. The X-ray Diffraction Intensity Curve of the PSA/MWCNTs Fibers.

FTIR Analysis of PSA/MWCNTs Fibers

The FTIR spectra of PSA/MWCNT nanofibers are show in *Figure 5*. The result shows that the MWCNT has few effects on the position and shape of peaks along the FTIR curve of PSA/MWCNTs fibers, indicating that the MWCNTs have no significant influences on the molecular structure and chemical composition of composite fibers.

The amide N-H stretching vibration occurred at 3351cm^{-1}. The characteristic peak at 1645cm^{-1} was amino link -C=O- stretching vibration absorption peak that is the absorption band of $\tilde{N}$. The characteristic peak at 1589 cm^{-1} is attributed to the

stretching vibration of -C-C-. Both the flexural vibrations of -NH- in -CONH- and the stretching vibration of -CN- correspond to the characteristic peak at about 1550 cm^{-1}. The absorption peak at about 1257cm^{-1} is the absorption band of $\acute{O}$, caused by coupled vibrations of -NH- and -C-N-. It indicates the presence of -CONH- in polymers. The characteristic peaks at 1321cm-1 and 1149cm-1 are caused by symmetrical stretching vibration and anti-symmetric stretching vibration of $–SO_2–$ respectively. Para replace characteristic peak of benzene ring occurs at 831cm^{-1}. It could be deduced that one of the components of the blended polymer/particle system is Polysulfonamide. In addition, there was a weak absorption peak detected at around 831cm^{-1} that is the characteristic peak of -C-Cl. The presence of this peak was because that acyl chloride and DMAC interacted, consuming monomer and producing CH_3Cl.

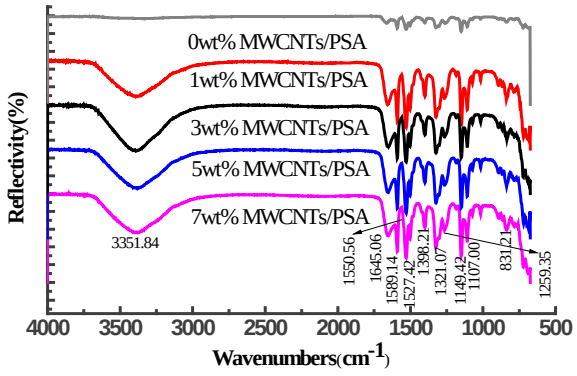

FIGURE 5. FTIR Curves of the electrospun PSA/MWCNTs fibers.

Electrical Conductivity of Fiber Mats

As illustrated in *Figure 6*, when the MWCNT concentration ranges from 1% to 5%, the surface specific resistance rate of the composite nano-fibers decreases, meanwhile the reduction amplitude increases gradually. However, there is an increase in surface specific resistance rate when the concentration of MWCNTs is over 5%. There are four parameters affecting the conductivity of the fiber mats: the conductive property of MWCNTs, MWCNT size, MWCNT concentration and MWCNT dispersion in polymer solution. The mechanism of MWCNT electrical conduction is related to the unpaired electron. Sp^2 hybridization occurs among carbon atoms and an unpaired electro of each carbon atom is on π orbit that is perpendicular to the layers. Therefore, MWCNTs show excellent conductivity properties. The addition of MWCNTs increases the conductivity of fibers. At low concentration, MWCNTs could be dispersed into solution by ultrasonic vibration and mechanical stirring, and most of the MWCNTs are isolated with each other, which limits the formation of a conductive network. Increasing the MWCNT concentration can increase the opportunity to connect with each other and shorten the distance among MWCNTs, favoring the formation of a conductive network. Therefore, at below 5% concentration, the surface specific resistance rate of nanocomposite fibers can be decreased with the addition of more and more MWCNT. However, at above 5% concentration, large agglomerates have been found (over 6mm in scale), it leads a severely decreasing of the conductivity of MWCNTs. In addition, some broken circuit occurs in the network due to agglomeration, the surface specific resistance rate increasing and the conductivity decreasing.

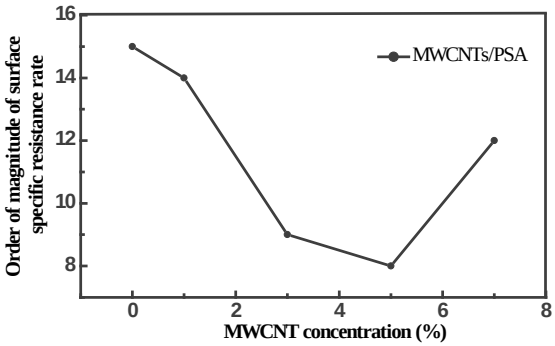

FIGURE 6. The surface specific resistance rate of PSA/MWCNTs fibers prepared with different MWCNT concentrations.

Mechanical Properties of Electrospun PSA/MWCNTs Nanofibers

The breaking tenacity of PSA/MWCNTs fibers with different MWCNT concentration is demonstrated in *Figure 7*. The results obtained show the addition of MWCNTs causes an increase in breaking tenacity before percolation threshold. The breaking tenacity of fibers can be improved gradually when the MWCNT concentration ranges from 1% to 3%. In contrast, when the concentration is over 3%, the crystallinity begins to decrease. The crystallinity can decrease to 0.306 when 7% MWCNT concentration, it is 23.3% lower in comparison with the electrospun PSA fibers. The main parameter affecting the breaking tenacity of fiber mats is the interface bonding state between the MWCNT and PSA matrix[41].

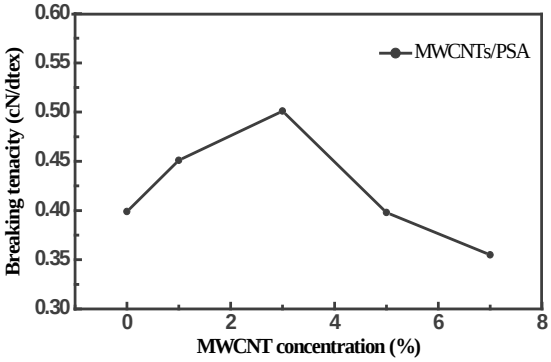

FIGURE 7. The breaking tenacity of the electrospun PSA/MWCNTs fibers with different MWCNT concentrations.

When the composite fibers are drawn from the PSA matrix under tension, usually some flaw will appear and continue to expand due to the poor breaking tenacity of PSA matrix until it meets MWCNTs blended inside the PSA matrix. At low concentration, MWCNTs could be dispersed uniformly in PSA matrix by ultrasonic vibration and mechanical stirring, wrapped with PSA matrix closely. When the MWCNTs debonding with the PSA matrix or itself occurs (*Figure 8a*), it dissipates energy. Therefore, the mechanical property can be improved. When the tension is increased further, the flaw expands along the MWCNTs until it reaches the weak regions between MWCNTs and the PSA matrix, and then the MWCNT can be extracted from the PSA matrix [42] as shown in *Figure 8b*. Energy must be dissipated during the separation of MWCNTs with the PSA matrix, thus it can improve the mechanism property of the composite fibers. Moreover, there are many interspaces and holes left in solution during the stirring of the spinning solution. MWCNTs may be embedded into these interspaces and holes, making the materials structure tighter and improving the breaking tenacity of fibers.

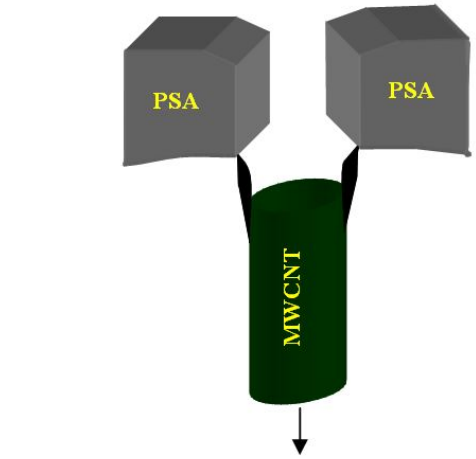

(a) MWCNT debonding from the PSA/MWCNTs interface layer

(b) PSA matrix debonding from the PSA/MWCNTs layer

FIGURE 8. The Failure Model of the PSA/MWCNTs composite fibers.

The Thermal Stability of Electro-spun PSA/MWCNTs Nanofibers

Figure 9 and *Figure 10* present the thermo-gravimetric (TG) curve and differential thermo-gravimetric curve (DTG) of PSA/MWCNTs nano-fibers with different MWCNT concentrations.

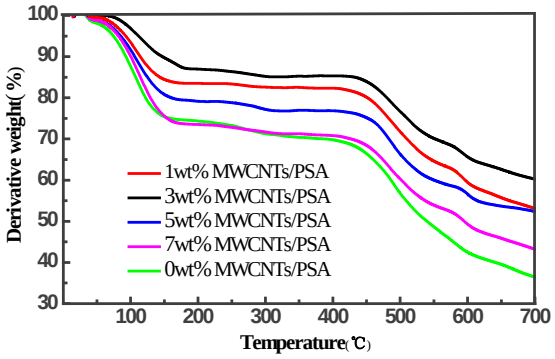

FIGURE 9. The TG curves of PSA/MWCNTs fibers with different MWCNT concentrations.

It can be observed that the thermal decomposition of PSA/MWCNTs samples is a decomposition process of mass loss. All the PSA/MWCNTs samples have a high mass loss rate at about 100℃ as shown in *Figure 10*. The reason is that samples are not dried before thermogravimetric test and there is some DMAC solvent and water left inside the samples. The volatilization of the DMAC solvent and water leads to a high mass loss rate.

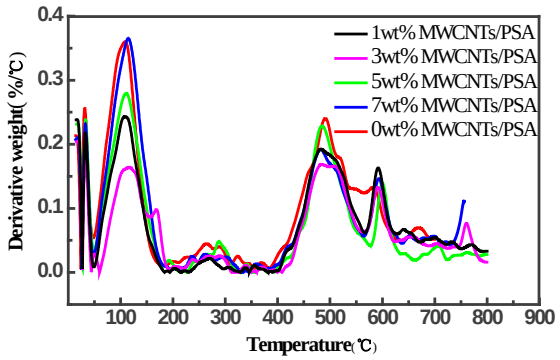

FIGURE 10. The DTG curve of PSA/MWCNTs fibers with different MWCNT concentrations.

Significant mass drop occurs between T_0 and 700 degrees. Macromolecular chains of the PSA polymer moved severely until the breakage accompanied with the release of small molecules and gas, leading to the mass loss. For example, at 500~600℃, macromolecular chains of PSA decompose at C-N section, and then SO_2, NH_3 and CO_2 will be released [43, 44]. The key thermal degradation indexes have been summarized in *Table II*.

TABLE II. Thermal characteristic parameters from TG and DTG curves of PSA/MWCNTs fibers

Sample	T_0/□	$d\alpha/dt$	T_{max}/□	α (%)
PSA	392.57	0.2401	491.22	36.48
1wt% MWCNTs / PSA	434.62	0.1925	482.56	53.10
3wt% MWCNTs / PSA	445.87	0.1688	483.50	60.23
5wt% MWCNTs / PSA	431.74	0.1924	481.83	52.34
7wt% MWCNTs / PSA	416.10	0.2288	484.93	43.63

T_0—the initial decomposition temperature;
$d\alpha/dt$ —the maximum thermal decomposition rate;
T_{max}/degree—the temperature of the maximum thermal decomposition rate;
α —the mass residual ration at 700 degrees.

The T_0 is defined as the initial decomposition temperature at which the change of accumulation mass can be detected by the thermal-balance. It represents the temperature that TG curve begins to deviate from the baseline [45]. The results obtained from *Table II* show that the addition of MWCNTs considerably delays the decomposition time of fibers, and increases the mass residual ratio at 700 degrees, improving the initial decomposition temperature of fibers effectively. In addition, it is interesting to find that the T_0 order of the samples is 3wt%MWCNTs/PSA>1wt%MWCNTs/PSA> 5wt%MWCNTs/PSA>7wt%MWCNTs/PSA, which indicates that the order of the thermostability is 3wt%MWCNTs/PSA>1wt%MWCNTs/PSA>5wt% MWCNTs/PSA>7wt%MWCNTs/PSA. It attributes to the dispersion of MWCNTs in PSA matrix. At low concentration, MWCNTs could be dispersed in PSA matrix by the ultrasonic vibration and mechanical stirring. Moreover, the MWCNTs in this work have been treated using acid and there are many - OH hydrophilic group on their surface, leading to a tight coupling with the matrix. The effective bonding between MWCNTs and PSA matrix limits the movement of PSA molecular chains and favors the formation of a thermally stable network by which the heat could be delivered, the thermo stability of the fibers can be improved considerably. However, at a high concentration, MWCNTs could not be dispersed homogenously in matrix and large agglomerates have been found, the thermal network of PSA/MWCNTs system is not established well and thus the thermostability of fibers decreases.

CONCLUSION

PSA/MWCNTs composite fibers with different concentrations of MWCNTs were electrospun in this research. The effects of MWCNTs on the morphology and properties of fibers were investigated. Our experimental results can be summarized as follows: (1) the addition of MWCNTs can lead to an increase of the average diameter of PSA fibers and lead to a more roughly fiber surface. The fiber average diameter increases slightly as the MWCNT concentration increases from 1% to 5%; (2) The addition of MWCNTs decreases the crystallinity of the PSA fibers; (3) The conductivity of PSA fibers increases gradually when the MWCNT concentration increases from 1% to 5%; (4) An increase of the fiber mechanical properties can be observed with an increasing of the MWCNT concentration below 3% MWCNT. Over 3% MWCNT, the breaking tenacity of the PSA fibers decreases. At 7% MWCNT concentration, the mechanical strength of the PSA /MWCNTs fiber could be even less than that of the electrospun pure PSA fibers; (5) The MWCNTs can improve the thermostability of the fibers effectively.

ACKNOWLEDGMENTS

This work was supported by the Excellent Young Teachers Program of Shanghai Municipal Education Commission (gjd10013); Technological Innovation Fund of Shangtex Holding (Group) Corporation (2011-zx-03-2); Graduate students Innovation Fund of Shanghai University of Engineering Science (2011yjs42);Visiting Scholarship Program funded by the China Scholarship Council(CSC).

REFERENCES

[1] Nandana, Bhardwaj; Subhas C, Kundu; Electrospinning: A fascinating fiber fabrication technique, Biotechnology Advances, Vol. 28, 2010, pp. 325–347.

[2] Greiner, A.; Wendorff, J.H.; Electrospinning: A fascinating method for the preparation of ultrafine fibers, Angewandte Chemie-International Edition, Vol. 46, 2007, pp. 5670-5730.

[3] Keun Hyung Lee; Hak Yong Kim; Young Jun Ryu; Mechanical behavior of electrospun fiber mats of poly(vinyl chloride)/polyurethane polyblends, Journal of Polymer Science Part B: Polymer Physics, Vol. 41, pp. 1256-1262.

[4] Ming Tian; Yi Gao; Yi Liu; Bis-GMA/TEGDMA dental composites reinforced with electrospun nylon 6 nanocomposite nanofibers containing highly aligned fibrillar silicate single crystals, Polymer, Vol. 48, 2007, pp. 2720–2728.

[5] Wang Xianfeng; Ding Bin; Yu Jianyong; A highly Sensitive Humidity Sensor Based on a Nanofibrous Membrane Coated Quartz Crystal Microbalance. Nanotechnology, Vol. 21, 2010, pp. 055502.

[6] Song Xiaofeng; Wang Zhaojie; Liu Yongben; A Highly Sensitive ethanol Sensor Based on Mesoporous ZnO - SnO2 nanofiers, Nanotechnology, Vol. 20, 2009, pp. 075501.

[7] Wu Wanuu; Ting Jyhming; Huang Pojung; Electrospun ZnO nanowires as gas sensors for ethanol detection, Nanoscale Res Lett, Vol. 4, 2009, pp. 513-517.

[8] Chae, S.K.; Park, H.; Yoon, J.; Polydiacetylene supramolecules in electrospun microfibers: Fabrication, micropatterning, and sensor applications, Advanced Materials, Vol. 19, 2007, pp. 521-524.

[9] Choi Seung-Hoon; Ankonina Guy; Youn Doo-Young; Hollow ZnO Nanofibers Fabricated Using Electrospun Polymer Templates and Their Electronic Transport Properties, ACS Nano, Vol. 3, 2009, pp. 2623-2631.

[10] Wang Xianfeng; Ding Bin; Yu Jianyong; Electro-netting: Fabrication of two-dimensional nano-nets for highly sensitive trimethylamine sensing, Nanoscale, 2011, pp. 911-915.

[11] Uyar T.; Havelund R.; Hacaloglu J.; Functional electrospun polystyrene nanofibers incorporating alpha - , beta - , and gamma - cyclodextrins: comparison of molecular filter performance, ACS Nano, Vol. 4, 2010, pp. 5121-5130.

[12] Pitt Supaphol; Chidchanok Mit Uppatham; Manit Nithitanakul; Ultrafine electrospun polyamide-6 fibers: Effect of emitting electrode polarity on morphology and average fiber diameter, Journal of Polymer Science Part B: Polymer Physics, Vol. 43, 2005, pp. 3699-3712.

[13] Yoon K.; Kim K.; Wang X.F.; High flux ultrafiltration membranes based on electrospun nanofibrous PAN scaffolds and chitosan coating, Polymer, Vol 47, 2006, pp. 2434-2441.

[14] Ding Yu; Jia Wenzhao; Zang Heng; Carbonized Hemoglobin Nanofibers for Enhanced H2O2 Detection, Electroanalysis, Vol. 22, 2010, pp. 1911-1917.

[15] Sui Xiaomeng; Shao Changlu; Liu Yichun; Photoluminescence of polyethylene oxide–ZnO composite electrospun fibers, Polymer, Vol. 48, 2007, pp. 1459-1463.

[16] Tzeng Ping; Kuo Chi Ching; Lin Sung Tso; New Thermoresponsive Luminescent Electrospun Nanofibers Preparedfrom Poly [2,7-(9,9-dihexylfluorene)] -block-poly(N-isopropylacrylamide)/PMMABlends, Macromolecular Chemistry and Physics, Vol. 211, 2010, pp. 1408-1416.

[17] Lee Jung Ah; Krogman Kevin C.; Ma Minglin; Highly Reactive Multilayer-Assembled TiO2 Coating on Electrospun Polymer Nanofibers, Advanced Materials, Vol. 21, 2009. pp. 1252-1256.

[18] Ding B.; Li C.R.; Miyauchi Y.; Formation of novel 2D polymer nanowebs via electrospinning, Nanotechnology, Vol. 17, 2006, pp. 3685-3691.

[19] Salalha W.; Kuhn J.; Dror Y.; Encapsulation of bacteria and viruses in electrospun nanofibers, Nanotechnology, Vol. 17, 2006.

[20] Hong Y.L.; Chen X.S.; Jing X.B.; Fabrication and drug delivery of ultrathin mesoporous bioactive glass hollow fibers, Advanced Functional Materials, Vol. 20, 2010 pp. 1503-1510.

[21] Moncy V. Jose; Vinoy Thomas; Derrick R. Dean; Fabrication and characterization of aligned nanofibrous PLGA/Collagen blends as bone tissue scaffolds, Polymer, Vol. 50, 2009, pp. 3778–3785.
[22] Ashraf Sh.; Asran S.Henning; Goerg H. Michler; Polyvinyl alcohol–collagen–hydroxyapatite biocomposite nanofibrous scaffold: Mimicking the key features of natural bone at the nanoscale level, Polymer, Vol. 51, 2010, pp. 868–876.
[23] Byung-Moo Min; Sung Won Lee; Jung Nam Lim; Chitin and chitosan nanofibers: electrospinning of chitin and deacetylation of chitin nanofibers. Polymer, Vol. 45, 2004, pp. 7137-7142.
[24] Ki Hoon Lee; Chang Seok Ki; Doo Hyun Baek; Application of electrospun silk fibroin nanofibers as an immobilization support of enzyme, Fibers and Polymers, Vol. 6, 2005, pp. 181-185.
[25] Bayat Masoumeh; Yang Heejae; Ko Frank; Electromagnetic properties of electrospun Fe3O4/carbon composite nanofibers, Polymer, Vol. 52, 2011, pp. 1645-1653.
[26] Saeedeh Mazinani; Abdellah Ajji; Charles Dubois; Morphology, structure and properties of conductive PS/CNT nanocomposite electrospun mat. Polymer, Vol. 50, 2009, pp. 3329–3342.
[27] Sachiko Sukigara; Milind Gandhi; Jonathan Ayutsede; Regeneration of Bombyx mori silk by electrospinning—part 1: processing parameters and geometric properties. Polymer, Vol. 44, 2003, pp. 5721–5727.
[28] Sachiko Sukigara; Milind Gandhi; Jonathan Ayutsede; Regeneration of Bombyx mori silk by electrospinning. Part 2. Process optimization and empirical modeling using response surface methodology, Polymer, Vol. 45, 2004, pp. 3701–3708.
[29] Kenneth Kar Ho Wong; Martin Zinke-Allmang; Jeffery L. Hutter; The effect of carbon nanotube aspect ratio and loading on the elastic modulus of electrospun poly(vinyl alcohol)-carbon nanotube hybrid fibers, Carbon, Vol. 47, 2009, pp. 2571-2578.
[30] Kim G.M.; Michler G.H.; Pötschke P.; Deformation processes of ultrahigh porous multiwalled carbon nanotubes/polycarbonate composite fibers prepared by electrospinning, Polymer, Vol. 46, 2005, pp. 7346-7351.
[31] Wang M.; Hsieh A.J.; Rutledge G.C.; Electrospinning of poly(MMA-co-MAA) copolymers and their layered silicate nanocomposites for improved thermal properties, Polymer, Vol. 46, 2005, pp. 3407-3418.
[32] Zhou Weiping; Wu Yulong; Wei Fei; Elastic deformation of multiwalled carbon nanotubes in electrospun MWCNTs–PEO and MWCNTs–PVA nanofibers, Polymer, Vol. 46, 2005, pp. 12689-12695.
[33] Saeed Khalid; Park Soo Young; Lee Hwa Jeong; Preparation of electrospun nanofibers of carbon nanotube/polycaprolactone nanocomposite, Polymer, Vol. 47, 2006, pp. 8019-8025.
[34] Moncy V. Jose; Brian W. Steinert,; Vinoy Thomas; Morphology and mechanical properties of Nylon 6/MWNT nanofibers, Polymer, Vol. 48, 2007, pp. 1096-1104.
[35] Ra EJ; An KH; Kim KK; Anisotropic electrical conductivity of MWCNT/PAN nanofiber paper, Chemiccal Physics Letters, Vol. 413, 2005, pp. 188-193.
[36] Sen R.; Bin Z.; Perea D.; Preparation of single-walled carbon nanotube reinforced polystyrene and polyurethane nanofibers and membranes by electrospinning, Nano Letters, Vol. 4, 2004, pp. 459-64.
[37] Wang X.F.; Wang F.H.; Ren J.R.; Properties and application of PSA fiber, The development and application of conference proceedings of high-temperature PSA fiber in 2009. China Textile Engineering Society, Shanghai Textile Association, 2009, pp. 8-9.
[38] Mu W.M; Flame retardant fiber and fabric, Textile industry press: Beijing, 1990.
[39] J. F.; Properties and application of polysulfonamide fiber. Shanghai Textile Science & Technology, 1981, pp. 49-52.
[40] Baumgarten Peter K; Electrostatic spinning of acrylic microfibers, Journal of Colloid and Interface Science, Vol. 36, 1971, pp. 71-79.
[41] Zheng Yutao; Chen Jiuji; Cao Derong; The Technical Progress of Interfacial Compatibility between Modified Plant Fiber and Thermoplastic Composite Materials, Cellulose Science and Technology, Vol. 13, 2005, pp. 45-55.
[42] Hu Furong; Chen Guorong; Du Yongjuan; The Surface and Interface of Materials, East China University of Science and Technology Press: Shanghai, 2001.

[43] Linda J. Broadbelt; Andrew Chu; Michael T. Klein; Thermal stability and degradation of aromatic polyamides. Part 2 Structure-reactivity relationships in the pyrolysis and hydrolysis of benzamides, Polym Degrad Stab, Vol. 45, 1994, pp. 57-70.
[44] Linda J. Broadbelt; Andrew Chu; Michael T. Klein; Thermal stability and degradation of aromatic polyamides. Part 1 Pyrolysis and hydrolysis pathways, kinetics and mechanisms of N-phenyl benzamide, Polym Degrad Stab, Vol. 44, 1994, pp. 137-144.
[45] Zhang M.Z.; Liu B.J.; Gu X.Y.; Study method of polymer materials, China Light Industry Press: Beijing, China, Vol. 125, 2000.
[46] Xin, B.J., et al., Study on the thermal behaviour of polysulfonamide/multi-wall carbon nanotube composites. Journal of Industrial Textiles, 2013. 42(4): p. 434-445.
[47] Xin, B.J.; Chen Z.M. and Wu X.J.; Electrical conductivity of CNT/polysulfonamide composites. Journal of the Textile Institute, 2013. 104(4): p. 357-362.

AUTHORS' ADDRESSES

Bin-Jie Xin
Wenjie Chen
Shanghai University of Engineering Science
No 333, Longteng Road
Songjiang District
Shanghai 201620
CHINA